

All atom molecular dynamics simulations for unique compartmentalization in a peptide based hydrogel

6.1 INTRODUCTION

Hydrogels are important class of soft materials due to their broad-ranging functionalities and applications. Hydrogels have shown potent applications as super-absorbers, in the fields of medicines or biology [Peppas *et al.*, 2000; van der Linden *et al.*, 2004; El-Rehim, 2005; Pavlyuchenko *et al.*, 2009; Slaughter *et al.*, 2009; Fujimoto *et al.*, 2009]. The underlying structure of a polymeric hydrogel is based upon the cross-linking due to covalent bonds within the polymers and water molecules get trapped inside the hydrogel via cohesive forces [Estroff and Hamilton, 2004; Draper and Adams, 2017; Goodrich *et al.*, 2018]. Water molecules get absorbed within the vacant spaces among the polymer chains [Pal *et al.*, 2009]. Monomers which polymerize to form the cross-linked network lose their individual chemical properties as their covalent interactions are modified. This implies that even if the monomer unit is water soluble, the hydrogel formed via cross-linking of monomers, may be water insoluble.

In the last few decades, another class of hydrogels has emerged and has received noble attention as they have served as an agreeable alternate to polymeric hydrogels. This category of hydrogels is a supra-molecular network composed of small molecules [Estroff and Hamilton, 2004; Raeburn and Adams, 2015; Draper and Adams, 2017]. These small molecules self-assemble via non-covalent interactions and form fibrous structures. The fibres then connect via supra-molecular interactions leading to the formation of hydrogel which can trap water molecules. With respect to the polymeric hydrogels, the constituents of these hydrogels do not lose their physio-chemical identity [Estroff and Hamilton, 2004; Draper and Adams, 2017]. This is due to the non-covalent interactions which govern the self-assembly of the gel network. Hence, unlike the properties of polymeric hydrogels, the supra-molecular hydrogels can be easily dissolved. The process of dissolution leads to an increase in the entropy of the system and therefore, the mechanism is thermodynamically favorable [Draper and Adams, 2017]. Hence, to fully explore the potentials of this hydrogel, it is crucial to understand the key parameters which govern its physiological properties.

MD simulations have been widely accepted to gain an understanding of the gelation mechanism. This technique has noteworthy contributions in interpreting experimental results which sometimes seem to be implausible. MD simulations hold the capacity to deal with huge number of atoms, mainly arising from a large amount of solvent molecules in the system, to study the hydrogelation process [Karplus and McCammon, 2002]. In the previous studies, MD has shown a strong proficiency in understanding the controlling factors to obtain gels of desirable physical and mechanical properties. Water has an important role in hydrogelation as it is responsible for the solubility, integrity and diffusion of molecules, which is necessary for biomedical applications [Gun'ko *et al.*, 2017]. The local arrangement of water molecules near the hydrogel, their dynamical properties and diffusion have been analyzed by following their trajectories [Tamai *et al.*, 1996; Oldiges and Tönsing, 2000; Chiessi *et al.*, 2010]. Dynamics of water molecules staying inside the poly(vinyl alcohol) hydrogels have been studied by employing MD simulations [Chiessi *et al.*, 2005]. The diffusion co-efficients and residence times are determined from the mean square displacement of water and the values are in good agreement with the experimental findings. Anti-crude oil

adhesion properties are examined for PAAS-g-PVDF and PAA-g-PVDF hydrogels [Gao *et al.*, 2016]. The MSD and diffusion co-efficients of water molecules residing near the hydrogel surface reveal the slow movement of water molecules near PAAS-g-PVDF. With the formation of water layers near PAAS-g-PVDF, the energy barrier for water molecules to escape from the polyionized hydrogel is higher. Thus the confinement of water molecules near the hydrogel surface makes it oleophobic, i.e., due to adhering of water molecules onto the surface, the surface is protected from oils. Molecular dynamics based approaches have also enabled to study the processes of hydrogel swelling and transition in volume [Mann *et al.*, 2011; Walter *et al.*, 2012; Ou *et al.*, 2015]. MD based self assembly mechanism of hydrogels is carried out for peptide amphiphiles. It is seen that the hydrophobic and hydrophilic interactions, hydrogen bondings and temperature effects play crucial roles in the self-assembly of the constituent molecules [Fu *et al.*, 2013]. Another sub-category of non-covalent interactions, referred to as $\pi - \pi$ interactions, has been reported to play a major role in self assembly of hydrogels such as in dipeptide Fmoc-D-ala-D-ala [Zhang *et al.*, 2013] and in surfactant-free ionene polymers [Bachl *et al.*, 2014].

In this chapter, an MD based study has been reported for a small peptide-conjugate based supra-molecular hydrogel, PyKC. Experiments have shown no dissolution of the hydrogel in water or in other solvents for a period over than a year [Singha *et al.*, 2019]. Further, even at a low concentration of 0.005 wt%, the emission spectra of the hydrogel shows an excimer band at ~ 475 nm which indicates the presence of π - π stacking which is also confirmed by an upfield shift in NMR signals. The monomer unit of this peptide gets dimerized in presence of water via disulfide formation which further leads to the hydrogel formation. The process of hydrogelation via dimerization is experimentally verified using dithiothreitol (DTT), which is known to break the disulfide linkage. It is found that in the presence of DTT, no hydrogel formation takes place and thus dimerization is critical for the hydrogelation mechanism. This hydrogel is found to be highly effective in protecting the enzymes from denaturing agents like heat, methanol or urea for a long time. The insolubility of PyKC is supremely exceptional and an unusual property as compared to the solubilities of other supra-molecular hydrogels in water/solvents. To obtain a molecular level understanding on the unique properties of PyKC dimer in water, all-atom molecular dynamics simulations are performed.

The structure of a folded and an open chain PyKC dimer considered in this study is shown in figure 6.1. Binding energies of the two dimers of PyKC are computed from the electronic structure calculations to determine the favorable conformation of stacked PyKC dimers. The energetically favorable PyKC dimer is chosen as the initial structure of the dimer for MD simulations in water. The work reveals the role of hydrogen bonding and $\pi - \pi$ stacking in acquiring a special supra-molecular arrangement which is responsible for the insolubility and a unique compartmentalization capacity of this hydrogel. An understanding of such an exceptional feature of a hydrogel can be utilized in the fields of material sciences, medicines or biology.

6.2 COMPUTATIONAL DETAILS

6.2.1 Electronic structure calculations

Structures of the open and folded conformations of PyKC are obtained using Chemdraw and are shown in figure 6.1(a, b). These configurations are used as the initial configuration for the geometry optimization which are carried out using DFTB+ package [Aradi *et al.*, 2007]. The geometry optimized structure of the PyKC dimer is obtained by using density functional tight binding (DFTB-D3) [Koskinen and Mäkinen, 2009; Grimme *et al.*, 2010, 2011] method. The DFTB method implements minimal atom-centered Slater-type all-valence basis sets. It also uses the approximate Hamiltonian matrix which is based on the DFTB energy equation. The electrostatic interactions originating due to the partial charges are evaluated using self-consistent charges (SCC). The effect of dispersion terms is included to consider the role of van der Waals interactions and the

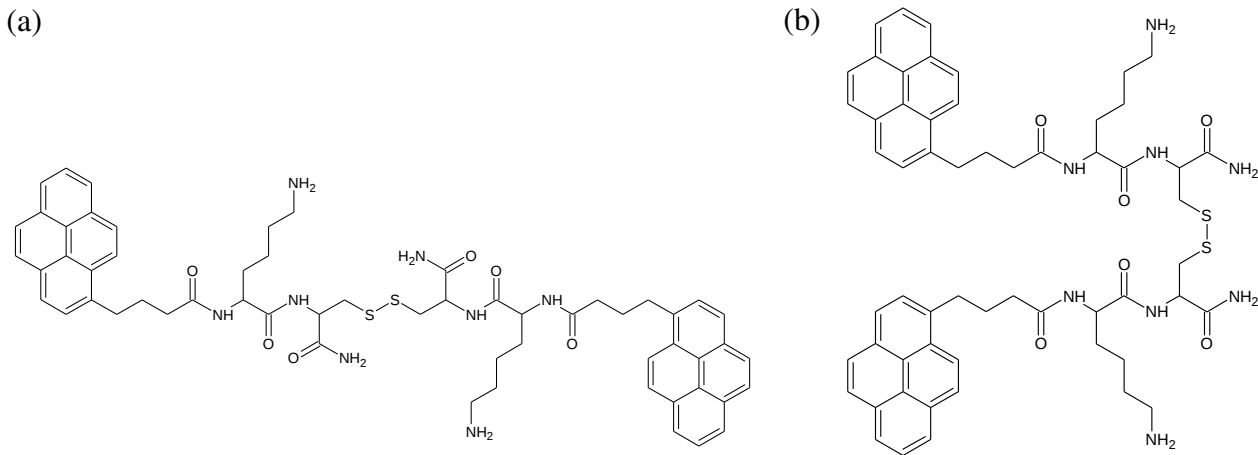


Figure 6.1: (a) Open and (b) Folded PyKC dimer conformers drawn using ChemDraw. These two structures are the initial configurations for the geometry optimization.

effect of $\pi - \pi$ stackings. Element pair interactions of C, H and N are attained from the Standard DFTB parameters. Previous studies have shown the utility of DFTB in calculating the $\pi - \pi$ stacking energy for pyrene moiety based systems [Nénon and Champagne, 2013; Guo *et al.*, 2013]. The total DFTB energy (E_{Tot}) is computed using the following equation,

$$E_{Tot} = E_{BS} + E_{coul}[\delta n] + E_{rep}(R) \quad (6.1)$$

where E_{BS} , $E_{coul}[\delta n]$ and $E_{rep}(R)$ represent band structure energy, energy due to charge fluctuation and repulsive energy due to ion-ion interaction respectively. The PyKC dimers with open and folded conformations are optimized with dispersion correction terms. The geometries are optimized within a convergence criteria of 20000 steps. Once the geometries are optimized, each of the final configurations of the folded and the open PyKC dimers are separately stacked on top of one another in a way such that the planar pyrene rings remain parallel. The initial stacked configuration of open and folded PyKC dimers are shown in figure 6.2 (a) and (b) respectively. The snapshots of the geometry optimized open and folded dimers are shown in figure 6.2(c) and (d) in the presence of dispersion correction terms. The stacking energies (ΔE_{BE}) of the stacked dimers are computed using equation,

$$\Delta E_{BE} = E_{DE} - 2E_{ME} \quad (6.2)$$

where E_{DE} and E_{ME} signify the dimer and monomer energy respectively. The energies of the geometry optimized monomers, dimers and their binding energies are tabulated under table 6.1. From the table, it can be seen that the stacking or the binding energy of the folded conformer is higher than the corresponding open conformer, indicating it to be more stable. Since the $\pi - \pi$ stacking plays an important role in the stabilizing the supra-structures, for e.g. in DNA, protein folding or drug binding [Israelachvili *et al.*, 1977; Sinnokrot and Sherrill, 2006], hence, the folded conformer is chosen as the initial structure to perform all-atom MD simulations.

6.2.2 Molecular dynamics simulations

All the MD simulations for PyKC systems are carried out using GROMACS v4.6.5 [Bekker *et al.*, 1993; Abraham *et al.*, 2018; Lindahl *et al.*, 2001; Berendsen *et al.*, 1995; van der Spoel *et al.*, 2005; Hess *et al.*, 2008; Pronk *et al.*, 2013; Páll *et al.*, 2015; Abraham *et al.*, 2015]. The experimental results have shown that the critical concentration above which PyKC forms a self-supported hydrogel is 1 wt.% [Singha *et al.*, 2019]. Simulations are performed for folded

PyKC dimers and the rationale for selecting the folded conformer over the open conformation is based on the MD simulation of open conformers in water. Two open-chain dimers are solvated in water which spontaneously adopt a folded conformation within 10 ns in an NPT ensemble (figure A3 in the appendix). Hence simulations are carried out for a system having 60 dimers of the geometry optimized folded PyKC inserted in a cubic box. The concentration is held constant at 43.4 wt. % and the simulation is carried out using the SPC/E water model [Mark and Nilsson, 2001]. The bonded parameters for the folded PyKC-dimer are taken using the Automated topology builder(ATB) server [Malde *et al.*, 2011]. The non-bonded parameters are taken from GROMOS54a7 force-field [Schmid *et al.*, 2011]. The system is energy minimized with steepest descent algorithm [Leach, 2001]. This is followed by 100 ps NVT simulations where the temperature is held constant at 300 K using velocity rescale thermostat [Bussi *et al.*, 2007b]. Once the system reaches at thermal equilibrium, 42.5 ns NPT simulation is carried out. The pressure of the system is held constant at 1 bar using Parrinello-Rahman barostat [Parrinello and Rahman, 1981; Nosé and Klein, 1983]. A coupling constant of 1 ps is used to couple the system with the barostat. A time step of 2 fs is utilized for the simulation and the trajectories are saved at every 10 ps. Periodic boundary conditions are applied in each xyz-directions. The non-bonded interactions are computed within a cut-off distance of 1 nm whereas the Particle Mesh Ewald (PME) method is used to treat the Coulombic interactions [Ewald, 1921]. All analyses are performed for the last 5.5 ns run length and are discussed in the next sections.

To compare water dynamics confined near PyKC with bulk water (BW), a box of SPC/E water is simulated for 2 ns. The simulation is performed in an NPT ensemble using 2 fs time step. The temperature and pressure are maintained at 300 K and 1 bar using Nosé-Hoover thermostat [Nosé, 1984; Hoover, 1985] and Parrinello-Rahman barostat respectively [Parrinello and Rahman, 1981; Nosé and Klein, 1983]. Once the system is equilibrated, a 5 ns NVT simulation is performed using a time step of 0.4 fs with velocity rescale thermostat [Bussi *et al.*, 2007b] using a coupling constant of 2 ps. To capture the hydrogen bond dynamics, small time steps are required. Hydrogen bond lifetimes are typically in ps time scale. Thus, to capture the hydrogen bond dynamics of bulk water and trapped water molecules, we have used a time of 0.4 fs. The non-bonded interactions are computed within a cut-off distance of 0.9 nm. The length of the simulation box is 1.87 nm in all three directions. All analyses to understand the BW dynamics are performed for the last 60 ps of the simulation.

6.3 RESULTS AND DISCUSSIONS

Stability of PyKC conformers from DFTB

The experimental results have reported the insolubility and a unique confinement of the PyKC-hydrogel [Singha *et al.*, 2019]. To understand this behavior, a molecular level study of the building blocks of the hydrogel is required. The study is initiated by obtaining the most stable PyKC conformer. For this, the geometry optimization of open and folded PyKC dimers are carried out considering the dispersion correction terms. Using these configurations, the stacked structures of both open and folded PyKC dimers are created. The dimers are stacked in such a manner that their pyrene rings stay parallel. Both the stacked configurations are geometry optimized following similar protocols as for the non-stacked configurations. The geometry optimized configurations of the stacked dimers using dispersion corrections are shown in figure 6.2(c) and (d).

The electronic structure calculations give the dispersion energies and total energies of the geometry optimized PyKC dimers which are summarized under table 6.1. Next, the binding energies of these stacked dimers are computed using equation 6.2. The stacking energies of the open and folded PyKC conformers are found to be -57.92 and -78.5 kcal mol⁻¹ respectively for configurations (c) and (d) in figure 6.1. Hence the folded conformer has more stability or energetically more

preferable over the open conformer. Figure 6.2(e) and (f) display the geometry optimized structures of folded PyKC dimer and a stacked folded dimer respectively. The closest inter-planar distance for

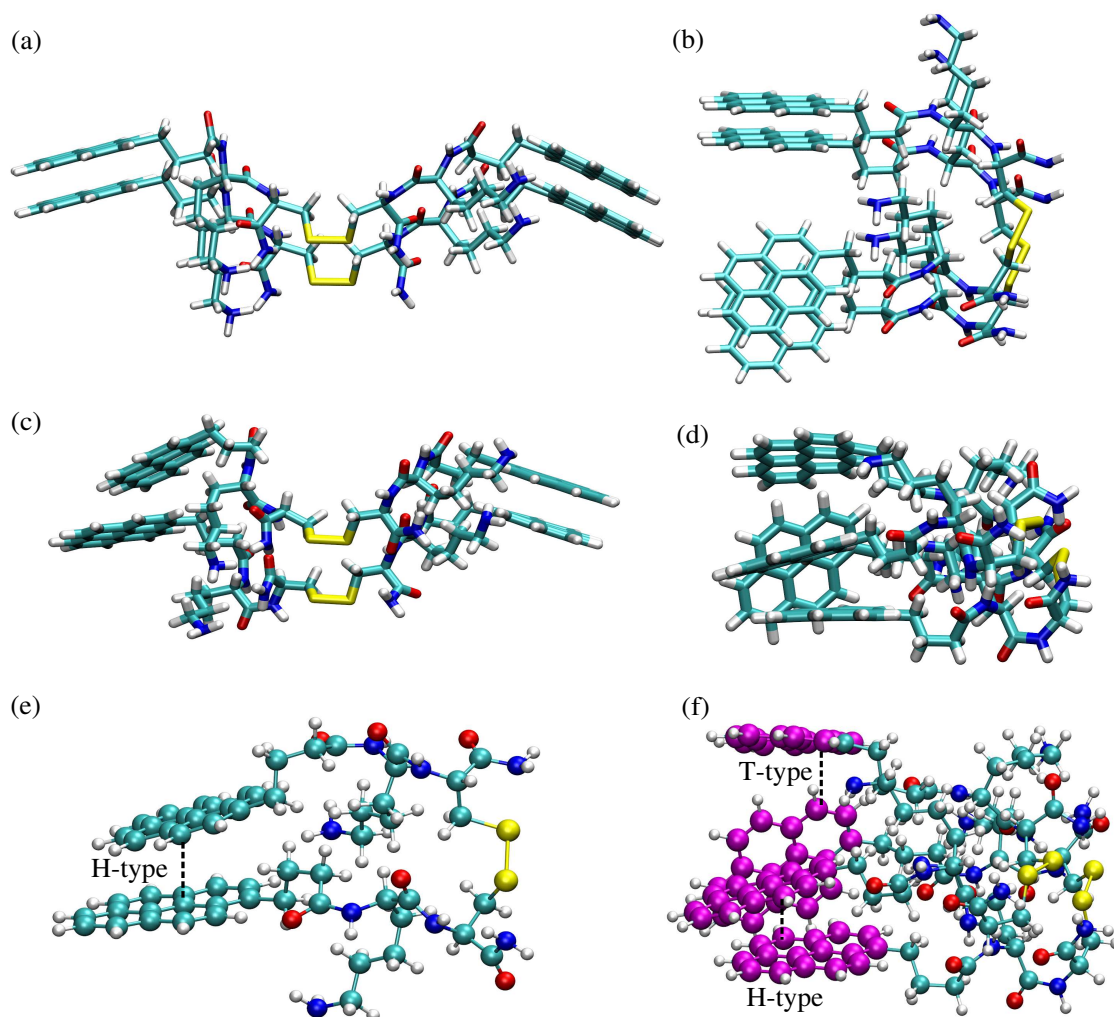


Figure 6.2: The initial stacked configurations of (a) open PyKC dimer and (b) folded PyKC dimer, configurations of stacked PyKC dimers obtained after geometry optimization using dispersion corrections for (c) open and (d) folded chains, (e) geometry optimized structure of folded PyKC dimer with dispersion correction. The pyrene rings stack in a parallel fashion and contribute towards $\pi - \pi$ stacking (H-type). (f) Snapshot of two stacked folded PyKC dimers obtained after the geometry optimization. For clarity, the pyrene rings are shown in magenta color. The rings participate in both H-type and T-type of $\pi - \pi$ stacking and thus have strong stacking energy.

the stacked dimer as obtained from DFTB is found to be 2.44 Å which agrees with the results found from the PXRD experiment [Singha *et al.*, 2019]. From figure 6.2(f), it is seen that the stacked folded PyKC dimer has both H-type and T-type of $\pi - \pi$ stacking. Hence the stability of the folded stacked dimer is attributed to both T-type and H-type of π -stacking interactions.

Unique compartmentalization of PyKC in water

The geometry optimized folded conformer is stable and used as the initial configuration for AA-MD simulations. The equilibration of the system is monitored by the time evolution of potential energy and SASA and shown in figure 6.3 (a) and (b) respectively. The final snapshot of the system obtained after 42.5 ns MD simulation is shown in figure 6.4. From the figure, it can be seen that

Table 6.1: Energies of the open and folded dimers, stacked dimers and their stacking energies obtained from the DFTB calculations. The folded PyKC conformer has a stronger stacking energy. The inter-planar distances obtained after DFTB geometry optimization and PXRD experiment [Singha *et al.*, 2019] are in good agreement indicating towards the presence of $\pi - \pi$ stacking.

Configuration	Energy (Hartree)				Stacking energy (ΔE_{BE}) kcal/mol	Inter-planar distance Å
	Dimer		Stacked dimer			
	Dispersion	Total	Dispersion	Total		
(a) Open	-0.255	-168.811	-0.571	-337.714	-57.92	2.96 (H-type)
(b) Folded	-0.275	-168.807	-0.607	-337.740	-78.50	2.44 (T-type)

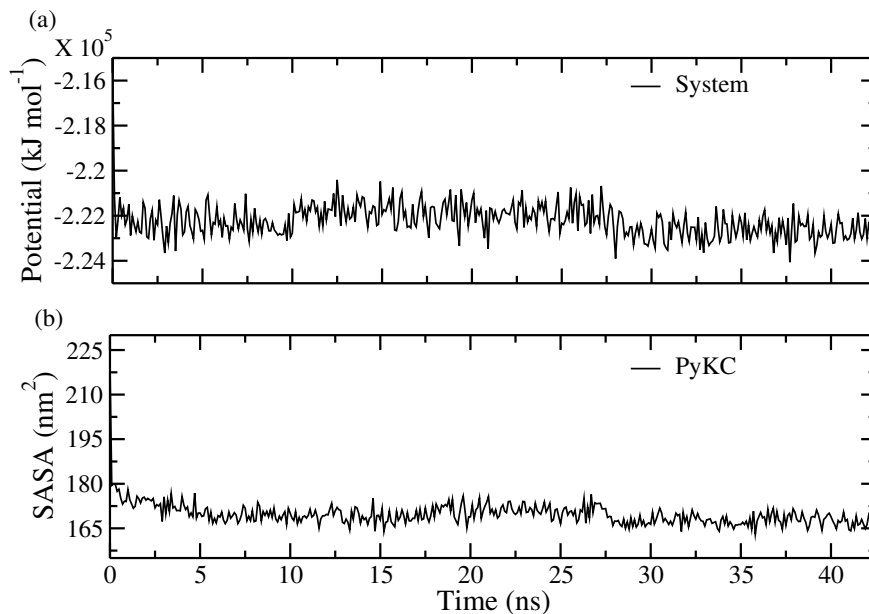


Figure 6.3: Time evolution of (a) potential energy and (b) solvent accessible surface area (SASA) to examine the equilibration for the system.

the PyKC-dimers self-assemble to form a layer-like structure with an interface between water and PyKC. The inset in the figure explains the molecular arrangement within the PyKC aggregates. The distance between the pyrene rings is ~ 0.34 nm which falls within the π stacking distance. The self-assembly is assisted by the intramolecular hydrogen bonds between nitrogen atoms (N) and oxygen atoms (O) of PyKC. The arrangement of water within the self-assembly is investigated by calculating the density profiles of water, pyrene rings and the PyKC shown in figure (6.5). The direction across the PyKC layers is taken as the normal vector. From figure 6.5, it is observed that there are distinct interfaces between PyKC layers and water molecules demonstrating the compartmentalization of water molecules and PyKC in the self-assembled structures. Interestingly, the densities reveal that there is a substantial amount of water inside the PyKC layers near the interfaces. These water molecules are referred to as trapped water (TW). The locations of pyrene and the hydrophilic N, O atoms show strong overlaps. The hydrophilic atoms are deeply buried within the hydrophobic pyrene moieties. The locations of hydrophilic atoms remaining buried inside is unlike the arrangements of hydrophilic atoms within the lipids or surfactants in the membranes or vesicles of biological relevance [Berkowitz *et al.*, 2006; Debnath *et al.*, 2009; Kanduč *et al.*, 2016; Baoukina *et al.*, 2017].

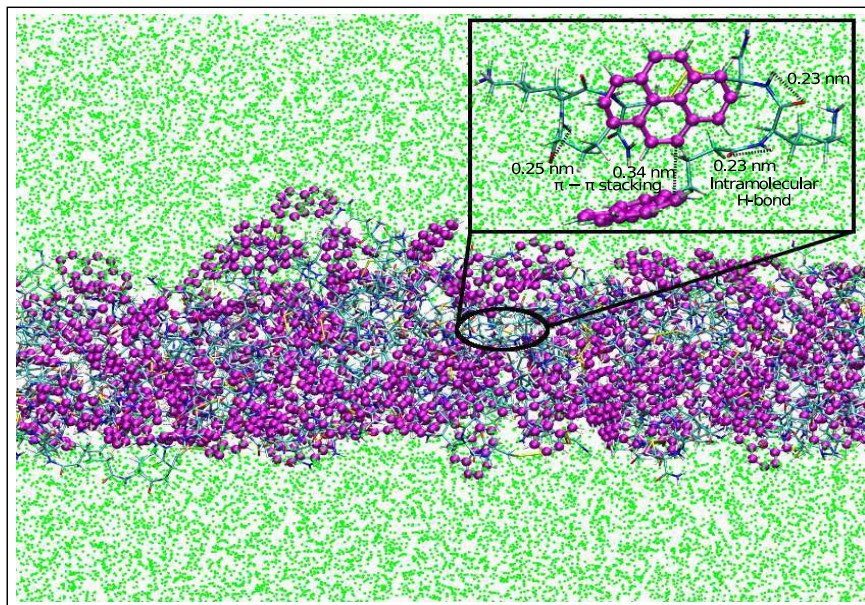


Figure 6.4: Snapshot of PyKC folded dimers in presence of water (green color) obtained from the MD simulation. Well-defined interfaces of water and PyKC can be seen which manifest the compartmentalization of PyKC and water. The inset in figure shows the intramolecular hydrogen bonding within the peptide conjugate and the $\pi - \pi$ stacking operating across the pyrene moieties which are responsible for the stability and self-assembly of PyKC in water.

The intra-molecular hydrogen bonds between N-H and O play important role in stabilizing the hydrophilic peptide conjugates. To investigate that, hydrogen bonds between these atoms are calculated. The geometric criteria to compute a hydrogen bond is based on two conditions, first the donor and acceptor distance is ~ 0.35 nm and the angle formed between the donor-H-acceptor is 30° [Luzar and Chandler, 1996b; Rey *et al.*, 2002; Lawrence and Skinner, 2003; Eaves *et al.*, 2005]. Following this geometric criteria, the number of intra-molecular hydrogen bonds between NH and O pairs is computed and is shown in figure 6.6 (a). It is seen that a large number of intra-molecular hydrogen bonds are formed between the hydrophilic pairs of NH and O. Trapped water molecules are stabilized within the PyKC domain due to the formation of inter-molecular H-bonds among themselves and with the amphiphilic groups of PyKC (figure 6.6(b)). Thus, they remain trapped because of two reasons: (a) formation of hydrogen bonds among the trapped water molecules, bonding between trapped water molecules and the NH or O groups of PyKC and (b) the pyrene rings acting as the hydrophobic barrier. Figure 6.7 shows the radial distribution function, $g(r)$, of the pyrene rings. The radial distribution function, as mentioned earlier, determines the local arrangement of atoms or moieties and is computed using following equation,

$$g(r) = \left\langle \frac{1}{\rho_N} \sum_{i=1}^N \sum_{j=1}^N \delta(r_{ij} - r) \right\rangle \quad (6.3)$$

where r_{ij} signifies the distances between the two particles i, j , N denotes the total number of particles, ρ signifies the mean particle density. The angle brackets denote the time averaging of $g(r)$. $g(r)$ of pyrene-pyrene reveals that the most probable distance between the pyrene rings is ~ 0.42 nm which is consistent with the $\pi - \pi$ stacking distance. Hence, the unique arrangement of PyKC hydrogel is attributed to $\pi - \pi$ stacking of pyrene moieties which act as a hydrophobic shield for the N/O atoms of the peptide-conjugate. The shielded components of the peptide-conjugate are thus restricted within the PyKC core and stabilize themselves via intra-molecular hydrogen bondings.

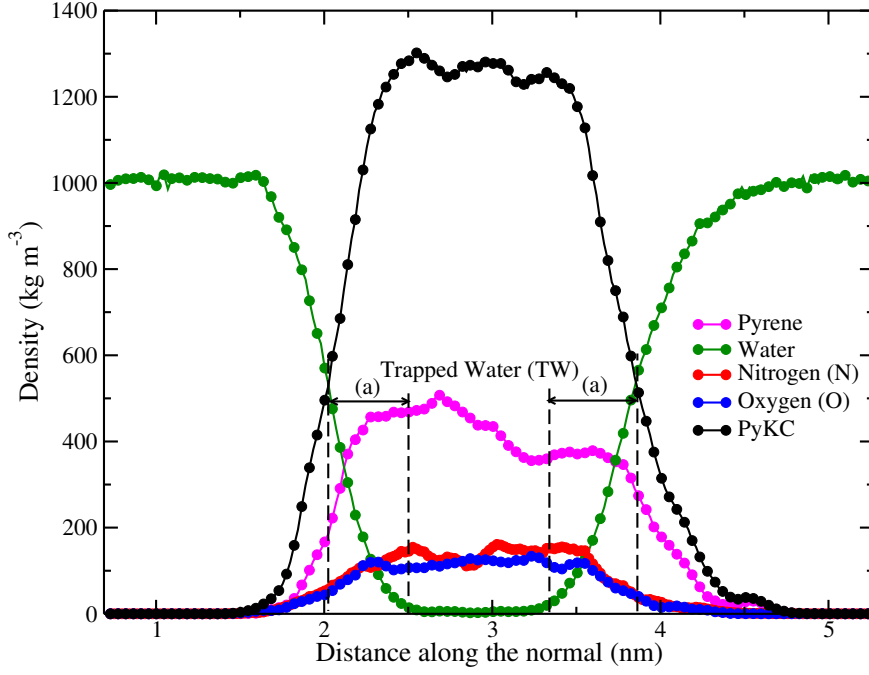


Figure 6.5: Density profile across the normal of PyKC layers obtained from MD simulation. Interfaces of PyKC and water layers are evident which show the presence of compartments of PyKC hydrogel and water. The hydrophilic atoms (N/O) of PyKC stay buried inside the layer and drive few water molecules into the core. The water molecules which continuously stay near the inner core of PyKC layer are referred to as trapped water (TW) and shown within the area designated as (a).

Slow dynamics of trapped water molecules (TW)

Since the hydrophilic atoms (N and O) are embedded within the PyKC layer, these atoms permit few water molecules to stay within the PyKC core and this class of water is mentioned as TW. A water molecule which stays in the PyKC core (shown as region (a) in the density profile) for a continuous period of 60 ps is classified as trapped water. The time of 60 ps time is chosen for defining the TW as the residence time of interface water molecules are ~ 100 ps [Debnath *et al.*, 2010; Srivastava and Debnath, 2018; Srivastava *et al.*, 2019]. To understand the dynamics of TW, the mean square displacement (MSD) is calculated using the equation,

$$\langle r^2(t) \rangle = \frac{1}{N} \sum_{i=1}^N \langle [r_i(t+t_o) - r_i(t_o)]^2 \rangle \quad (6.4)$$

where, summation is over all the molecules, t_o is time origin, t is the time, N denotes the total number of molecules and the angular brackets signify time averaging. The MSD for TW and BW are shown in figure 6.8. both the classes of water molecules. Generally, MSD follows the relation,

$$r^2(t) \sim Dt^\alpha \quad (6.5)$$

where D is the diffusion co-efficient, α denoted the anomalous diffusion exponent and t signifies the elapsed time. The values of α determine the type of diffusion viz. $\alpha < 1$ signifies sub-diffusion, $\alpha \sim 1$ denotes the process of diffusion and $\alpha > 1$ signifies super-diffusion. It is seen that dynamics of trapped water molecules is slower than the bulk water. The values of α calculated for TW and BW are found to be ~ 0.46 and ~ 0.93 respectively. This reveals that the TW molecules undergo a sub-diffusive dynamics and demonstrate the level of confinement.

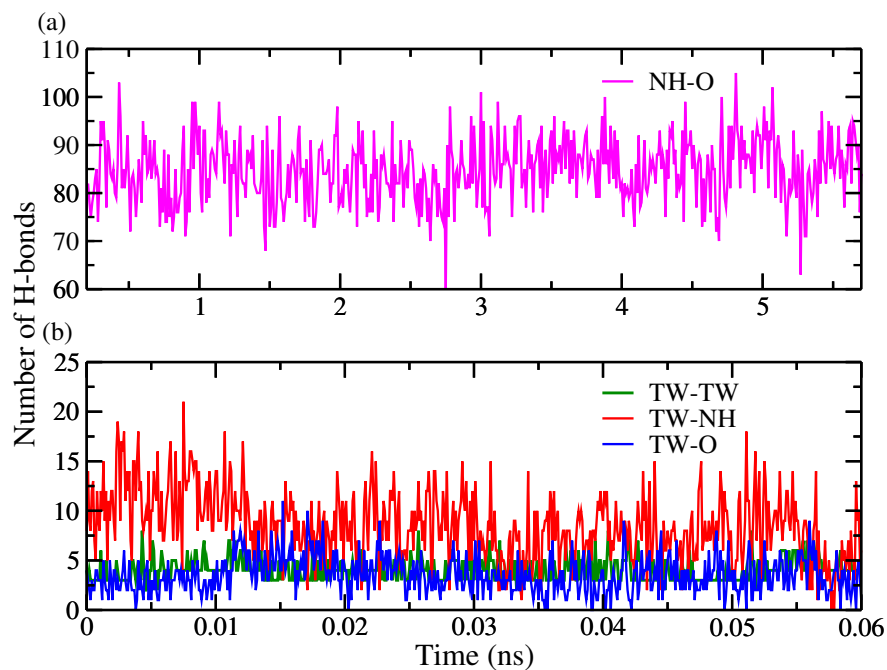


Figure 6.6: (a) Time evolution of the intramolecular hydrogen bonds between N and O atoms of PyKC are calculated for the production run which are responsible for the stability of the molecular arrangement of the hydrogel. (b) The time evolution of the intermolecular hydrogen bonds between trapped water molecules (TW-TW), and among the amphiphilic moieties of PyKC and trapped water molecules (TW-NH and TW-O). The intermolecular hydrogen bonds are computed for the time regime for which the TW molecules remain confined inside the PyKC core.

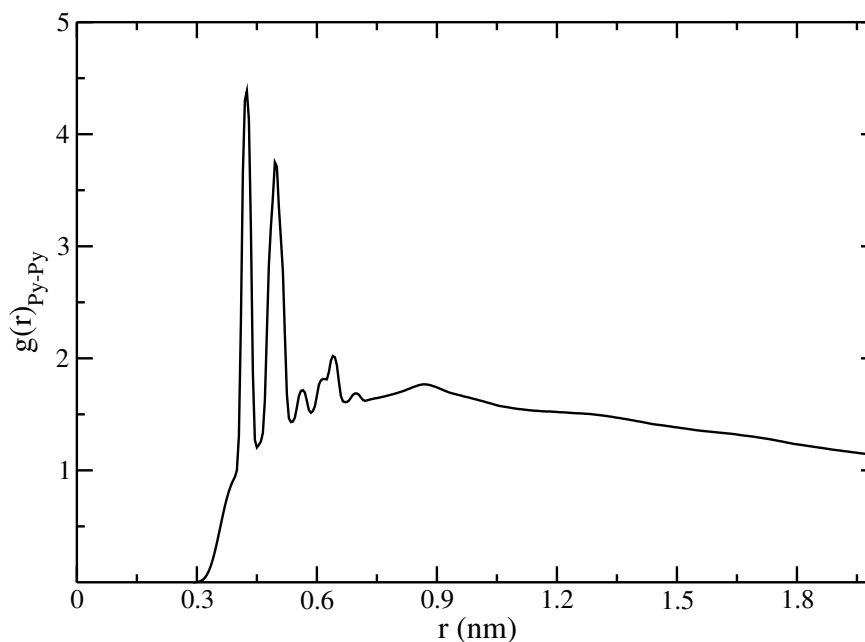


Figure 6.7: $g(r)$ of pyrene-pyrene determines the most probable location at ~ 0.42 nm which corresponds to the distance of $\pi - \pi$ interactions.

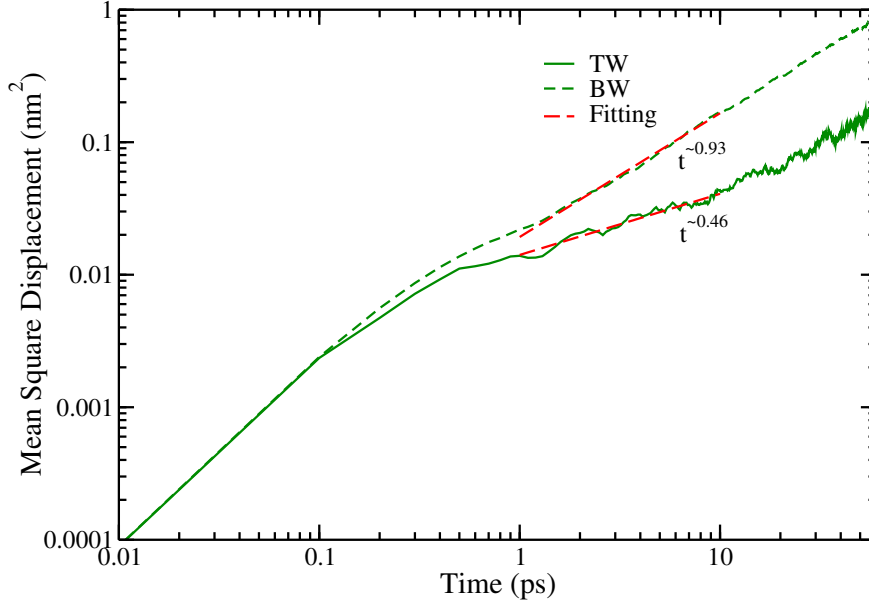


Figure 6.8: Comparison of mean square displacements of bulk water (BW) and trapped water (TW). BW obeys diffusive behavior whereas TW shows a sub-diffusive behavior which regards to the slow dynamics of trapped water molecules.

The intermittent hydrogen bond auto-correlation function is computed for both BW and TW and is shown in figure 6.9. It is calculated using the mathematical relation given below [Luzar and Chandler, 1996a; Chandra, 2000; Balasubramanian *et al.*, 2002],

$$C_{HB}(t) = \frac{\langle h_{TW-TW}(0)h_{TW-TW}(t) \rangle}{\langle h_{TW-TW} \rangle} \quad (6.6)$$

In the above equation, h_{TW-TW} denotes the hydrogen bonds between TW molecules and it is 1 if there exists a hydrogen bond, or else it is 0. From figure 6.9, it is identified that the relaxation of TW is much slower than the BW molecules. The change in activation free energy is measured by the reactive flux correlation analysis [Rey *et al.*, 2002]. The relaxation time (τ) of hydrogen bonding can be determined by using the forward rate constant (k) which signifies the hydrogen bond breaking phenomena as,

$$\tau = \frac{1}{k} \quad (6.7)$$

On assuming hydrogen bond breaking mechanism as an Eyring process, the Gibbs free energy, $\Delta G_{break}^\ddagger$, for breaking of the hydrogen bond is given as,

$$\tau = \frac{h}{k_B T} e^{\frac{\Delta G_{break}^\ddagger}{k_B T}} \quad (6.8)$$

In the above equation, h is the Planck's constant, k_B denotes the Boltzmann constant and T is the temperature. The energy ($\Delta G_{break}^\ddagger$) to break the hydrogen bond for TW is $11.06 \text{ kJ mol}^{-1}$ which is higher than that for the BW (8.27 kJ mol^{-1}). Similarly, the relaxation time, τ , for the TW is much slower than for the BW. The value of hydrogen bond relaxation for TW is comparable with the relaxation time for the water molecules confined near the biological surfaces [Srivastava and Debnath, 2018]. These results thus conclude that the significantly slow dynamics of trapped water molecules is due to the confinement of water molecules inside the PyKC layer. In experiments, aliquots from the bulk water are analyzed at different time-intervals and $\sim 5\%$ dissolution has been seen for 1 wt% PyKC hydrogel in water [Singha *et al.*, 2019]) Our results are in good agreement with the experimental results which dictate very less water transport across the PyKC hydrogel.

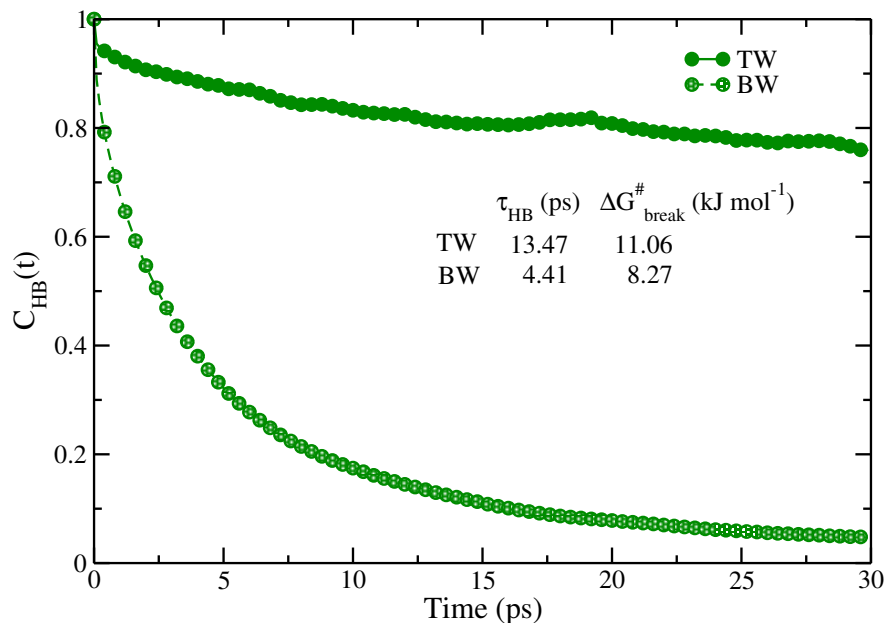


Figure 6.9: Hydrogen bond auto-correlation function ($C_{HB}(t)$) of trapped and bulk water molecules. Slow relaxation of TW is evident from the time variation of $C_{HB}(t)$. Longer relaxation time (τ_{HB}) and high activation energy for breaking of a hydrogen bond ($\Delta G_{break}^{\#}$) for TW lead towards a slow transport of water molecules across the supra-molecular hydrogel.

6.4 SUMMARY AND CONCLUSIONS

A unique compartmentalization property of a supra-molecular hydrogel composed of small PyKC molecules has been studied using molecular dynamics simulation. Experimental techniques employed on the hydrogel reveal its insolubility in water and other solutions for over more than a year. The mechanism of this exceptional property is studied at a molecular level using electronic structure calculations, followed by all-atom molecular dynamics (AA-MD) simulations. Geometry optimization using DFTB method using dispersion correction shows that a folded PyKC dimer is energetically more preferable over an open PyKC dimer. The stacked folded dimers exhibit strong stacking energy which is attributed to both T-type and H-type $\pi - \pi$ stacking arising from the pyrene-pyrene interactions of PyKC. The energetically favorable folded dimer is chosen for the starting configuration of MD simulations in presence of water. Simulations reveal that PyKC molecules self-assemble and form a network like structure leading to the formation of a hydrogel. The unusual ability of PyKC to function as a hydrogel is attributed to both $\pi - \pi$ interactions of pyrene moieties and the hydrogen bond formations. The hydrophilic components of the hydrogel are buried inside aromatic fragments and are stabilized via intramolecular hydrogen bonds and intermolecular hydrogen bonding with the trapped water molecules. Since the hydrophilic residues of PyKC are inside the core, they bring few water molecules along with them while self-assembling and are classified as trapped water molecules. These trapped water (TW) molecules do not get exchanged with the bulk water due to the hydrophobic shielding of pyrene rings. Also, water molecules which remain confined inside the core of the peptide conjugate follow sub-diffusive dynamics and form hydrogen bonds among themselves. The TW molecules have a slower relaxation time compared to that of the BW due to a higher Gibbs free energy for hydrogen bond breaking. Hence, the insolubility and the extraordinary compartmentalization tendency of PyKC hydrogel are due to the specific molecular arrangement of PyKC. The stability of the self-aggregated hydrogel is based on the non-covalent interactions like intramolecular hydrogen bonds among oxygen and nitrogen atoms and $\pi - \pi$ stackings among pyrene moieties. The transport of trapped water molecules is inhibited by the hydrogen bonds of trapped water molecules and the hydrophobic shielding due

to pyrene rings, resulting in a unique confinement in the system. Experiments conducted on PyKC hydrogels have shown that for tested solutes or solvents, there occurs no exchange to and from the PyKC hydrogel. This extraordinary confinement can be useful in various domains such as material science, tissue engineering, regenerative medicines and so on.

Publication: Nilotpal Singha, **Arpita Srivastava**, Bapan Pramanik, Sahnawaz Ahmed, Payel Dowari, Sumit Chowdhuri, Basab Kanti Das, Ananya Debnath and Debapratim Das, Unusual confinement properties of a water insoluble small peptide hydrogel **2019**, Chemical Science, *10*, 5920.